

Details of the disorder-induced transition between s_{\pm} and s_{++} states in the two-band model for Fe-based superconductors

V A Shestakov¹, M M Korshunov^{1,2} , Yu N Togushova²,
D V Efremov³  and O V Dolgov^{4,5} 

¹ Kirensky Institute of Physics, Federal Research Center KSC SB RAS, 660036, Krasnoyarsk, Russia

² Siberian Federal University, 660041, Krasnoyarsk, Russia

³ Leibniz-Institut für Festkörper- und Werkstofforschung, D-01069 Dresden, Germany

⁴ Max-Planck-Institut für Festkörperforschung, D-70569, Stuttgart, Germany

⁵ P.N. Lebedev Physical Institute RAS, 119991, Moscow, Russia

E-mail: mkor@iph.krasn.ru

Received 6 November 2017

Accepted for publication 4 January 2018

Published 31 January 2018



Abstract

Irradiation of superconductors with different particles is one of many ways to investigate the effects of disorder. Here we study the disorder-induced transition between s_{\pm} and s_{++} states in the two-band model for Fe-based superconductors with nonmagnetic impurities. Specifically, we investigate the important question of whether the superconducting gaps during the transition change smoothly or abruptly. We show that the behavior can be of either type and is controlled by the ratio of intraband to interband impurity scattering potentials, and by a parameter σ , that represents scattering strength and ranges from zero (Born approximation) to one (unitary limit). For the pure interband scattering potential and the scattering strength $\sigma \lesssim 0.11$, the $s_{\pm} \rightarrow s_{++}$ transition is accompanied by steep changes in the gaps, while for larger values of σ , the gaps change smoothly. The behavior of the gaps is characterized by steep changes at low temperatures, $T < 0.1T_{c0}$ with T_{c0} being the critical temperature in the clean limit, otherwise it changes gradually. The critical temperature T_c is always a smooth function of the scattering rate in spite of the steep changes in the behavior of the gaps.

Keywords: unconventional superconductors, iron pnictides, iron chalcogenides, impurity scattering

(Some figures may appear in colour only in the online journal)

1. Introduction

A number of physical properties of Fe-based materials reveal intriguing behavior. This includes unconventional superconductivity [1–6], transport coefficients and Raman spectra [7–10], magnetic and nematic states [11–14], and electronic band structure [15–19]. The first is of special interest because the transition temperature to the superconducting state (T_c) can be as high as 58 K in bulk materials [20] and up to 110 K in monolayer FeSe [21–25].

Except for extreme hole and electron dopings, the Fermi surface of Fe-based materials consists of two or three hole sheets around the $\Gamma = (0, 0)$ point and two electron sheets

around the $M = (\pi, \pi)$ point of the two-Fe Brillouin zone. Scattering between them with a large wave vector results in enhanced antiferromagnetic fluctuations, promoting the s_{\pm} type of the superconducting order parameter, which changes sign between electron and hole pockets [1, 3, 26]. On the other hand, bands near the Fermi level have mixed orbital content and orbital fluctuations, enhanced either by vertex corrections or the electron–phonon interaction may lead to the sign-preserving s_{++} state [27–31]. However, most experimental data—including observations of a spin-resonance peak in inelastic neutron scattering, a quasiparticle interference in tunneling experiments, and the NMR spin-lattice relaxation rate—support the s_{\pm} scenario [3, 6].

Superconducting states with different symmetries and different structures of order parameters act differently when subjected to disorder [32]. For instance, in a single-band s -wave superconductor, nonmagnetic impurities do not suppress T_c according to Anderson's theorem [33], while magnetic disorder causes T_c suppression at a rate following the Abrikosov-Gor'kov theory [34]. In unconventional superconductors, suppression of T_c as a function of a parameter Γ characterizing impurity scattering may follow quite a complicated law. Several experiments on Fe-based materials show that T_c suppression is much weaker than expected in the framework of the Abrikosov-Gor'kov theory for both nonmagnetic [35–41] and magnetic disorder [36, 42–45]. Many theoretical studies have revealed the importance of multiband effects in this matter; see [46–53]. One of the conclusions was that a system having the s_{\pm} state in the clean case may preserve a finite T_c in the presence of nonmagnetic disorder due to the transition to the s_{++} state. This was obtained both in the strong-coupling \mathcal{T} -matrix approximation [50] and via a numerical solution of Bogoliubov-de Gennes equations [54, 55].

The topology of the Fermi surface in Fe-based materials makes it sensible to use a two-band model as a compromise between maintaining simplicity and still allowing the possibility of capturing some essential physics. We have previously studied the $s_{\pm} \rightarrow s_{++}$ transition in such a model and shown that the transition can take place only in systems with a sizeable effective intraband pairing interaction [50]. The physical reason for the transition is quite clear, namely, if one of the two competing superconducting interactions leads to a state which is robust against impurity scattering, then although it was subdominating in the clean limit, it should become dominating while the other state is destroyed by the impurity scattering [32]. Here we focus on the details of the $s_{\pm} \rightarrow s_{++}$ transition. In particular, we are interested in the behavior of the superconducting gaps across the transition. We show that in the case of weak scattering (including the Born limit) at low temperatures, the gaps change steeply, while in all other cases they change smoothly across the transition.

2. Model

The Hamiltonian of the two-band model can be written in the following form:

$$H = \sum_{\mathbf{k}, \alpha, \sigma} \xi_{\mathbf{k}\alpha} c_{\mathbf{k}\alpha\sigma}^{\dagger} c_{\mathbf{k}\alpha\sigma} + \sum_{\mathbf{R}_i, \sigma, \alpha, \beta} \mathcal{U}_{\mathbf{R}_i}^{\alpha\beta} c_{\mathbf{R}_i\alpha\sigma}^{\dagger} c_{\mathbf{R}_i\beta\sigma} + H_{\text{sc}}, \quad (1)$$

where $c_{\mathbf{k}\alpha\sigma}$ is the annihilation operator of the electron with a momentum \mathbf{k} , spin σ , and band index α (or beta) that is equal to a (first band) or b (second band), and $\xi_{\mathbf{k}\alpha}$ is the quasiparticle dispersion that, for simplicity, we treat as linearized near the Fermi level. $\xi_{\mathbf{k}\alpha} = \mathbf{v}_{F\alpha}(\mathbf{k} - \mathbf{k}_{F\alpha})$, with $\mathbf{v}_{F\alpha}$ and $\mathbf{k}_{F\alpha}$ being the Fermi velocity and the Fermi momentum of the band α , respectively. The presence of disorder is described by the nonmagnetic impurity scattering potential \mathcal{U} at sites \mathbf{R}_i .

Superconductivity occurs in our system due to the interaction H_{sc} that in general can have different forms for

different pairing mechanisms. Hereafter we assume that the problem of finding the effective dynamical superconducting interaction is already solved, and both coupling constants and the bosonic spectral function are obtained. The latter describes the effective electron–electron interaction via an intermediate boson. In the case of local Coulomb (Hubbard) interactions [56, 57], intermediate excitations are spin or charge fluctuations [58], while in the case of electron–phonon interactions, these are phonons. The nature of the effective dynamical interaction is not important for the analysis which follows; of importance is rather that the corresponding bosonic spectral function peaks at some low frequency and drops down as frequency increases. To check whether the steepness is an intrinsic feature or there is another competitive phase requires calculation of the free energy that is beyond the scope of the present paper.

3. Method

Here we employ the Eliashberg approach for multiband superconductors [59]. The Dyson equation, $\hat{\mathbf{G}}(\mathbf{k}, \omega_n) = [\hat{\mathbf{G}}_0^{-1}(\mathbf{k}, \omega_n) - \hat{\Sigma}(\mathbf{k}, \omega_n)]^{-1}$, establishes the connection between the full Green's function $\hat{\mathbf{G}}(\mathbf{k}, \omega_n)$, the 'bare' Green's function (without interelectron interactions and impurities),

$$\hat{\mathbf{G}}_0^{\alpha\beta}(\mathbf{k}, \omega_n) = [i\omega_n \hat{\tau}_0 \otimes \hat{\sigma}_0 - \xi_{\mathbf{k}\alpha} \hat{\tau}_3 \otimes \hat{\sigma}_0]^{-1} \delta_{\alpha\beta} \quad (2)$$

and the self-energy matrix $\hat{\Sigma}(\mathbf{k}, \omega_n)$. Green's function for the quasiparticle with momentum \mathbf{k} and Matsubara frequency $\omega_n = (2n + 1)\pi T$ is a matrix in the band space (indicated by bold face) and in Nambu space (indicated by a hat). The latter is denoted by Pauli matrices $\hat{\tau}_i$.

In what follows, we assume that the self-energy does not depend on the wave vector \mathbf{k} but we keep the dependence on frequency and band indices:

$$\hat{\Sigma}(\omega_n) = \sum_{i=0}^3 \Sigma_{(i)\alpha\beta}(\omega_n) \hat{\tau}_i. \quad (3)$$

In this case, the problem can be simplified by averaging over \mathbf{k} . Thus, all equations will be written in terms of quasiclassical ξ -integrated Green's functions represented by 4×4 matrices in Nambu and band spaces,

$$\hat{\mathbf{g}}(\omega_n) = \int d\xi \hat{\mathbf{G}}(\mathbf{k}, \omega_n) = \begin{pmatrix} \hat{g}_{an} & 0 \\ 0 & \hat{g}_{bn} \end{pmatrix}, \quad (4)$$

where

$$\hat{g}_{\alpha n} = g_{0\alpha n} \hat{\tau}_0 + g_{2\alpha n} \hat{\tau}_2. \quad (5)$$

Here, $g_{0\alpha n}$ and $g_{2\alpha n}$ are the normal and anomalous (Gor'kov) ξ -integrated Green's functions in the Nambu representation,

$$g_{0\alpha n} = -\frac{i\pi N_{\alpha} \tilde{\omega}_{\alpha n}}{\sqrt{\tilde{\omega}_{\alpha n}^2 + \tilde{\phi}_{\alpha n}^2}}, \quad g_{2\alpha n} = -\frac{\pi N_{\alpha} \tilde{\phi}_{\alpha n}}{\sqrt{\tilde{\omega}_{\alpha n}^2 + \tilde{\phi}_{\alpha n}^2}}. \quad (6)$$

They depend on the density of states per spin at the Fermi level of the corresponding band ($N_{a,b}$), and on the renormalized (by the self-energy) order parameter $\tilde{\phi}_{\alpha n}$ and frequency $\tilde{\omega}_{\alpha n}$,

$$i\tilde{\omega}_{\alpha n} = i\omega_n - \Sigma_{0\alpha}(\omega_n) - \Sigma_{0\alpha}^{\text{imp}}(\omega_n), \quad (7)$$

$$\tilde{\phi}_{\alpha n} = \Sigma_{2\alpha}(\omega_n) + \Sigma_{2\alpha}^{\text{imp}}(\omega_n). \quad (8)$$

Often, it is convenient to introduce the renormalization factor $Z_{\alpha n} = \tilde{\omega}_{\alpha n}/\omega_n$ that enters the gap function $\Delta_{\alpha n} = \tilde{\phi}_{\alpha n}/Z_{\alpha n}$. It is the gap function that generates peculiarities in the density of states.

A part of the self-energy due to spin fluctuations or any other retarded interaction (electron–phonon, or retarded Coulomb interaction) can be written in the following form:

$$\Sigma_{0\alpha}(\omega_n) = T \sum_{\omega'_n, \beta} \lambda_{\alpha\beta}^Z(n - n') \frac{g_{0\beta n'}}{N_\beta}, \quad (9)$$

$$\Sigma_{2\alpha}(\omega_n) = -T \sum_{\omega'_n, \beta} \lambda_{\alpha\beta}^\phi(n - n') \frac{g_{2\beta n'}}{N_\beta}. \quad (10)$$

Coupling functions,

$$\lambda_{\alpha\beta}^{\phi, Z}(n - n') = 2\lambda_{\alpha\beta}^{\phi, Z} \int_0^\infty d\Omega \frac{\Omega B(\Omega)}{(\omega_n - \omega_{n'})^2 + \Omega^2}, \quad (11)$$

depend on coupling constants $\lambda_{\alpha\beta}^{\phi, Z}$ (which include density of states N_β in themselves) and on the normalized bosonic spectral function $B(\Omega)$ [60–62]. The matrix elements $\lambda_{\alpha\beta}^\phi$ can be positive (attractive) as well as negative (repulsive) due to the interplay between spin fluctuations and electron–phonon coupling [58, 60], while the matrix elements $\lambda_{\alpha\beta}^Z$ are always positive. For simplicity we set $\lambda_{\alpha\beta}^Z = |\lambda_{\alpha\beta}^\phi| \equiv |\lambda_{\alpha\beta}|$ and neglect possible anisotropy in each order parameter $\tilde{\phi}_{\alpha n}$.

We use a noncrossing, or \mathcal{T} -matrix, approximation to calculate the impurity self-energy $\hat{\Sigma}^{\text{imp}}$:

$$\hat{\Sigma}^{\text{imp}}(\omega_n) = n_{\text{imp}} \hat{\mathbf{U}} + \hat{\mathbf{U}} \hat{\mathbf{g}}(\omega_n) \hat{\Sigma}^{\text{imp}}(\omega_n), \quad (12)$$

where n_{imp} is the concentration of impurities and $\hat{\mathbf{U}}$ is the matrix of the impurity potential. The latter is equal to $\hat{\mathbf{U}} = \mathbf{U} \otimes \hat{\tau}_3$, where $(\mathbf{U})_{\alpha\beta} = \mathcal{U}_{\mathbf{R}_i}^{\alpha\beta}$. Without loss of generality we set $\mathbf{R}_i = 0$ for the single impurity problem studied here. For simplicity, the intraband and interband parts of the impurity potential are set equal to v and u , respectively, such that $(\mathbf{U})_{\alpha\beta} = (v - u)\delta_{\alpha\beta} + u$. The relation between the two will be controlled by the parameter η :

$$v = u\eta. \quad (13)$$

There are two important limiting cases: the Born limit (weak scattering) with $\pi u N_{a,b} \ll 1$ and the opposite case of a very strong impurity scattering (a unitary limit) with $\pi u N_{a,b} \gg 1$. With this in mind, it is convenient to introduce the scattering strength (generalized cross-section) parameter

$$\sigma = \frac{\pi^2 N_a N_b u^2}{1 + \pi^2 N_a N_b u^2} \rightarrow \begin{cases} 0, & \text{Born} \\ 1, & \text{unitary} \end{cases} \quad (14)$$

and the impurity scattering rate

$$\Gamma_{a,b} = \frac{2n_{\text{imp}}\sigma}{\pi N_{a,b}} \rightarrow \begin{cases} 2n_{\text{imp}}\pi N_{b,a}u^2, & \text{Born} \\ 2n_{\text{imp}}/(\pi N_{a,b}), & \text{unitary} \end{cases} \quad (15)$$

The procedure for further calculations is the following: i) solve equation (12), ii) calculate renormalizations of frequency (7) and order parameter (8) self-consistently, iii) use them to obtain Green's functions (6) and, consequently, (4).

To determine T_c , we solve linearized equations for the order parameter and the frequency,

$$\sum_{\omega'_n, \beta} \left[\delta_{nn'} \delta_{\alpha\beta} - \delta_{nn'} \tilde{\Gamma}_{\alpha\beta} \frac{\text{sgn}(\omega_{n'})}{|\tilde{\omega}_{\beta n'}|} - \pi T_c \sum_{\omega'_n, \beta} \lambda_{\alpha\beta}(n - n') \frac{\text{sgn}(\omega_{n'})}{|\tilde{\omega}_{\beta n'}|} \right] \tilde{\phi}_{\beta n'} = 0, \quad (16)$$

$$\tilde{\omega}_{\alpha n} = \omega_n + \sum_{\beta} \tilde{\Gamma}_{\alpha\beta} \text{sgn}(\omega_n) + \pi T_c \sum_{\omega'_n, \beta} |\lambda_{\alpha\beta}(n - n')| \text{sgn}(\omega_{n'}). \quad (17)$$

Here $\tilde{\Gamma}_{\alpha\beta}$ are the components of the impurity scattering rate matrix [50],

$$\tilde{\Gamma}_{ab(ba)} = \frac{\Gamma_{a(b)}(1 - \sigma)}{\sigma(1 - \sigma)\eta^2 N^2/(N_a N_b) + (\sigma\eta^2 - 1)^2}, \quad (18)$$

where $N = N_a + N_b$ is the total density of states in the normal phase. Note that the diagonal terms, $\tilde{\Gamma}_{aa}$ and $\tilde{\Gamma}_{bb}$, are absent in equations (16) and (17). Equation (16) can be written in matrix form as $\hat{\mathbf{K}}\tilde{\phi} = 0$, where $\hat{\mathbf{K}}$ and $\tilde{\phi}$ are a matrix and a vector, respectively, in the combined band and Matsubara frequency spaces. By varying T_c as a parameter, we determine its value as a point where the sign of $\det|\hat{\mathbf{K}}|$ changes.

4. Results

Here we choose the relation between densities of states as $N_b/N_a = 2$, and the following coupling constants: $(\lambda_{aa}, \lambda_{ab}, \lambda_{ba}, \lambda_{bb}) = (3, -0.2, -0.1, 0.5)$. This gives the s_{\pm} state with the superconducting critical temperature T_{c0} of 40 K in the clean limit [50, 61, 62] and the positive averaged coupling constant $\langle\lambda\rangle > 0$ where $\langle\lambda\rangle \equiv (\lambda_{aa} + \lambda_{ab})N_a/N + (\lambda_{ba} + \lambda_{bb})N_b/N$ [50].

Since we are interested in the behavior of gaps across the $s_{\pm} \rightarrow s_{++}$ transition, in figure 1 we plot $\Delta_{\alpha n}$ for the first Matsubara frequency $n = 0$ as functions of Γ_a at $T = 0.03T_{c0}$.

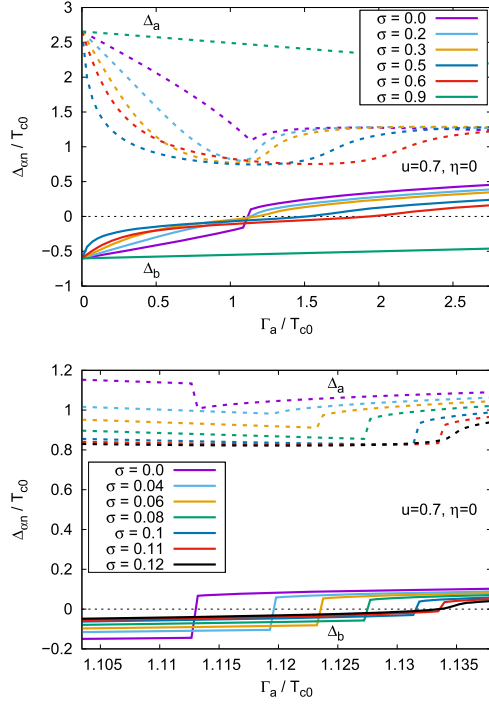


Figure 1. The first Matsubara gaps' $\Delta_{an=0}$ dependence on the nonmagnetic impurity scattering rate Γ_a for the s_{\pm} state with $\eta = 0$ and $T = 0.03T_{c0}$. In the upper panel, we show a wide range of σ 's, while the data in the lower panel demonstrate a jump in gaps at the point of the $s_{\pm} \rightarrow s_{++}$ transition for small values of σ . Note the smooth behavior of gaps for $\sigma > 0.11$.

Following the b -band behavior, we observe the transition for $\Gamma_a \gtrsim 1.1T_{c0}$. While for large values of η the gaps change smoothly across zero, for $\sigma < 0.12$ we notice a jump in the smaller gap Δ_{bn} when it crosses zero. It happens even in the Born limit $\sigma = 0$. At the same time, critical temperature is always a smooth function of Γ_a (see the T_c plot in figure 2). Critical temperature seems to 'not care' about the jump occurring in the behavior of the smaller gap. To understand why this happens, we studied the temperature evolution of gaps. Results for $\sigma = 0$ and $\eta = 0$ are shown in figure 3. Apparently, with increasing temperature, the steep behavior of Δ_{bn} changes to smooth dependence on the scattering rate. This happens at $T \sim 0.1T_{c0}$ and, naturally, at higher temperatures, including T_c , the system shows smooth behavior. We have checked that the temperature dependence of gaps shown in figure 3 stays the same for $\eta = 0.5$ and $\eta = 1$.

It is known that the strongest T_c suppression takes place in the Born limit with $\eta = 0$, while in the opposite limit of pure intraband scattering with $u = 0$ ($\eta \rightarrow \infty$), pairbreaking is absent because $\tilde{\Gamma}_{ab} \rightarrow 0$ [32]. A similar situation is also characteristic of the unitary limit with $\sigma = 1$ (see equation (18)).

To demonstrate how the transition evolves with the increasing intraband part of the impurity potential, v , in figures 4 and 5 we show results for different values of η at $T = 0.03T_{c0}$. Thus, in figure 4, we go from almost pure interband to uniform scattering. Apparently, the critical Γ_a at

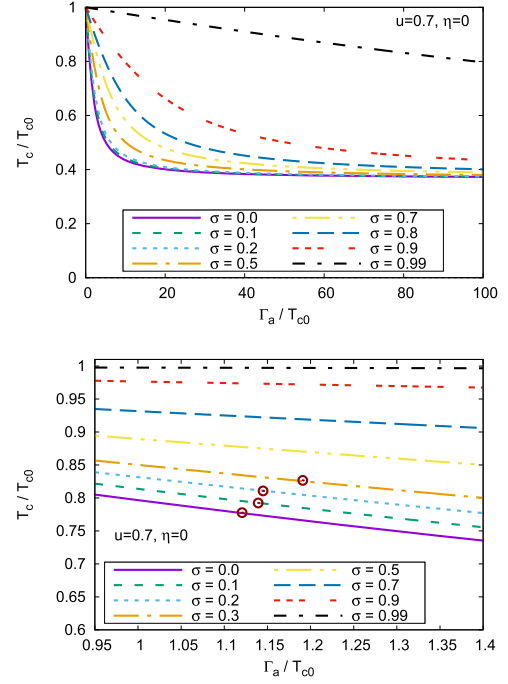


Figure 2. T_c versus Γ_a for the s_{\pm} state with $\eta = 0$. Results for a wide range of Γ_a 's is shown in the upper panel. In the lower panel, we show a narrow range of Γ_a 's where the $s_{\pm} \rightarrow s_{++}$ transition with jumps in gaps takes place. T_c shows smooth behavior at the transition points, which are marked by circles.

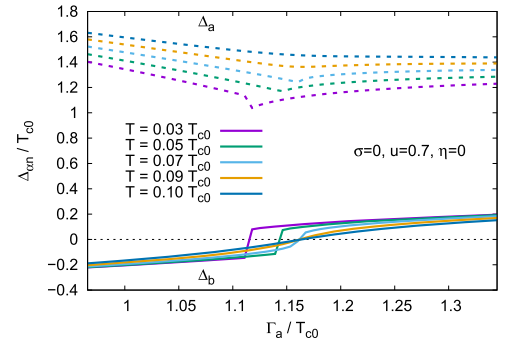


Figure 3. Temperature evolution of Matsubara gaps $\Delta_{an=0}$ for a range of Γ_a 's with $\sigma = 0$ and $\eta = 0$. Note the steep changes in behavior for smaller gaps at low temperatures and the restoration of smooth behavior for $T \gtrsim 0.09T_{c0}$.

which the transition takes place increases with increasing v for $\sigma > 0$. In the Born limit, we observe the jump in the gaps for all η 's at exactly the same critical Γ_a (see figure 5(a)).

5. Conclusions

Here we studied the details of the $s_{\pm} \rightarrow s_{++}$ transition in the two-band model for nonmagnetic impurity scattering in Fe-based superconductors. We show that the gaps change smoothly across the transition for all values of the cross-section parameter σ and intra- to interband impurity potentials ratio η , except for the case of weak scattering with small

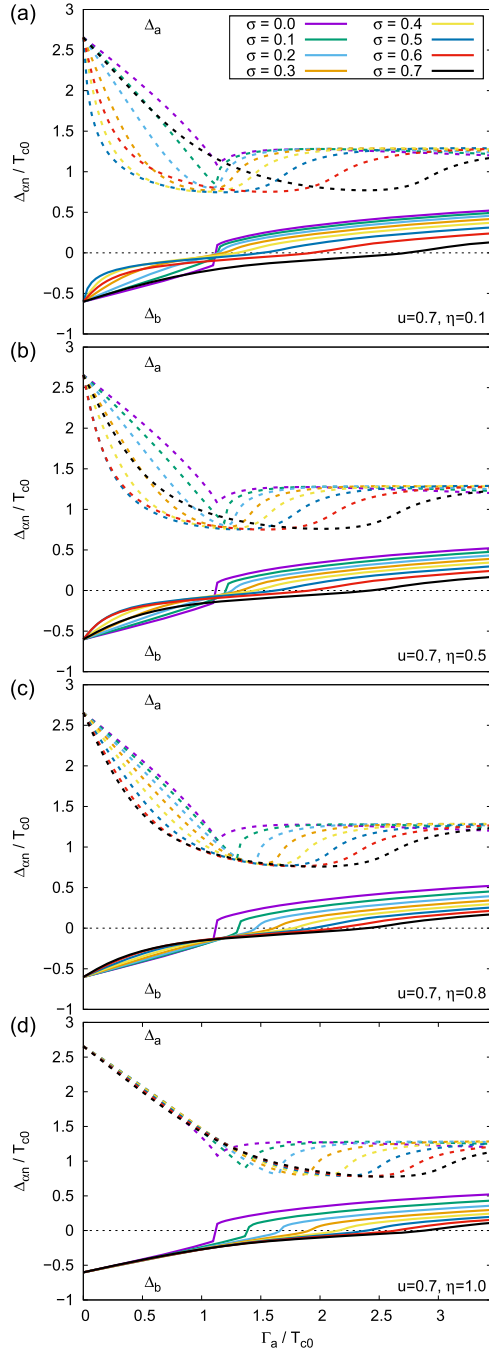


Figure 4. Matsubara gaps $\Delta_{\alpha n=0}$ versus Γ_a in the s_{\pm} state for various values of η , i.e. (a) $v = 0.1u$, (b) $v = u/2$, (c) $v = 0.8u$, and (d) uniform impurity potential $v = u$.

values of σ . In the latter case, the smaller gap changes steeply at the transition point. For larger scattering rate Γ_a , the smaller gap evolves smoothly. The behavior changes around $\sigma = 0.11$. With increasing temperature, the behavior of the gaps changes from the steep to the smooth at around $T \sim 0.1T_{c0}$ for all values of σ and η . That is the reason why the critical temperature is always a smooth function of the scattering rate and is not affected by the steep changes in the behavior of the gaps. The steepness is fragile and goes away if parameters are changed. We can not answer here the question whether the steep changes are intrinsic to the system or there

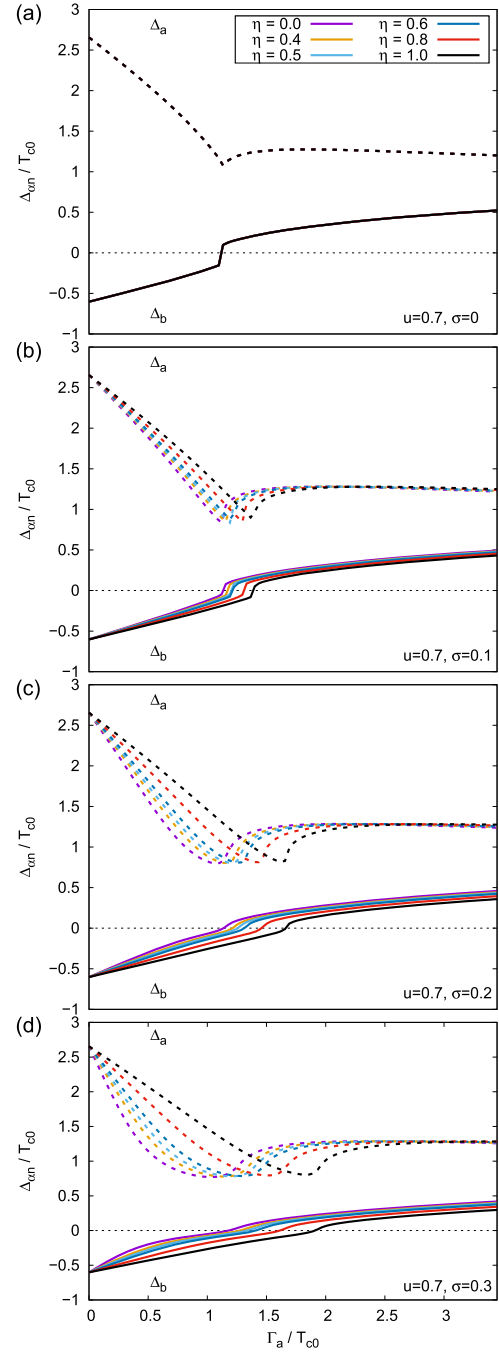


Figure 5. Matsubara gaps $\Delta_{\alpha n=0}$ versus Γ_a in the s_{\pm} state with varying η for (a) $\sigma = 0$, (b) $\sigma = 0.1$, (c) $\sigma = 0.2$, and (d) $\sigma = 0.3$. In panel (a), all curves for different η overlap.

is another competitive phase. Finding an answer requires calculation of the free energy and finding its minimum that is a separate complicated task.

Acknowledgments

We are grateful to P D Grigor'ev and M V Sadovskii for useful discussions. This work was supported in part by the Russian Foundation for Basic Research (grant 16-02-00098) and Government Support of the Leading Scientific Schools of

the Russian Federation (NSh-7559.2016.2). MMK and VAS acknowledge the support of the 'BASIS' Foundation for Development of Theoretical Physics and Mathematics.

ORCID iDs

M M Korshunov  <https://orcid.org/0000-0001-9355-2872>

D V Efremov  <https://orcid.org/0000-0002-1991-2056>

References

- [1] Mazin I I 2010 *Nature* **464** 183–6
- [2] Sadovskii M V 2008 *Phys.-Usp.* **51** 1201–27
- [3] Hirschfeld P J, Korshunov M M and Mazin I I 2011 *Rep. Prog. Phys.* **74** 124508
- [4] Reid J P *et al* 2012 *Supercond. Sci. Technol.* **25** 084013
- [5] Hosono H and Kuroki K 2015 *Physica C* **514** 399–422
- [6] Hirschfeld P J 2016 *C. R. Phys.* **17** 197–231
- [7] Stewart G R 2011 *Rev. Mod. Phys.* **83** 1589–652
- [8] Muschler B, Prestel W, Hackl R, Devereaux T P, Analytis J G, Chu J H and Fisher I R 2009 *Phys. Rev. B* **80** 180510
- [9] Canfield P C and Bud'ko S L 2010 *Annu. Rev. Condens. Matter Phys.* **1** 27–50
- [10] Kemper A F, Korshunov M M, Devereaux T P, Fry J N, Cheng H P and Hirschfeld P J 2011 *Phys. Rev. B* **83** 184516
- [11] Lumsden M D and Christianson A D 2010 *J. Phys.: Condens. Matter* **22** 203203
- [12] Fisher I R, Degiorgi L and Shen Z X 2011 *Rep. Prog. Phys.* **74** 124506
- [13] Dai P 2015 *Rev. Mod. Phys.* **87** 855–96
- [14] Inosov D S 2016 *C. R. Phys.* **17** 60–89
- [15] Ding H *et al* 2008 *Europhys. Lett.* **83** 47001
- [16] Richard P, Sato T, Nakayama K, Takahashi T and Ding H 2011 *Rep. Prog. Phys.* **74** 124512
- [17] Kordyuk A A 2012 *Low Temp. Phys.* **38** 888–99
- [18] Zi-Rong Y, Yan Z, Bin-Ping X and Dong-Lai F 2013 *Chin. Phys. B* **22** 087407
- [19] Kordyuk A A 2015 *Low Temp. Phys.* **41** 319–41
- [20] Fujioka M, Denholme S J, Tanaka M, Takeya H, Yamaguchi T and Takano Y 2014 *Appl. Phys. Lett.* **105** 102602
- [21] Qing-Yan W *et al* 2012 *Chin. Phys. Lett.* **29** 037402
- [22] Liu D *et al* 2012 *Nat. Commun.* **3** 931
- [23] He S *et al* 2013 *Nat. Mater.* **12** 605–10
- [24] Tan S *et al* 2013 *Nat. Mater.* **12** 634–40
- [25] Ge J F, Liu Z L, Liu C, Gao C L, Qian D, Xue Q K, Liu Y and Jia J F 2015 *Nat. Mater.* **14** 285–9
- [26] Korshunov M M 2014 *Phys.-Usp.* **57** 813–9
- [27] Kontani H and Onari S 2010 *Phys. Rev. Lett.* **104** 157001
- [28] Bang Y, Choi H Y and Won H 2009 *Phys. Rev. B* **79** 054529
- [29] Onari S and Kontani H 2012 *Phys. Rev. B* **85** 134507
- [30] Onari S and Kontani H 2012 *Phys. Rev. Lett.* **109** 137001
- [31] Yamakawa Y and Kontani H 2017 *Phys. Rev. B* **96** 045130
- [32] Korshunov M M, Togushova Y N and Dolgov O V 2016 *J. Supercond. Nov. Magn.* **29** 1089–95
- [33] Anderson P 1959 *J. Phys. Chem. Solids* **11** 26–30
- [34] Abrikosov A A and Gor'kov L P 1961 *Sov. Phys. - JETP* **12** 1243–53
- [35] Karkin A E, Werner J, Behr G and Goshchitskii B N 2009 *Phys. Rev. B* **80** 174512
- [36] Cheng P, Shen B, Hu J and Wen H H 2010 *Phys. Rev. B* **81** 174529
- [37] Li Y, Tong J, Tao Q, Feng C, Cao G, Chen W, chun Zhang F and Xu Z 2012 *New J. Phys.* **12** 083008
- [38] Nakajima Y, Taen T, Tsuchiya Y, Tamegai T, Kitamura H and Murakami T 2010 *Phys. Rev. B* **82** 220504
- [39] Tropeano M *et al* 2010 *Phys. Rev. B* **81** 184504
- [40] Kim H, Tanatar M A, Liu Y, Sims Z C, Zhang C, Dai P, Lograsso T A and Prozorov R 2014 *Phys. Rev. B* **89** 174519
- [41] Prozorov R, Kończykowski M, Tanatar M A, Thaler A, Bud'ko S L, Canfield P C, Mishra V and Hirschfeld P J 2014 *Phys. Rev. X* **4** 041032
- [42] Tarantini C *et al* 2010 *Phys. Rev. Lett.* **104** 087002
- [43] Tan D *et al* 2011 *Phys. Rev. B* **84** 014502
- [44] Grinenko V *et al* 2011 *Phys. Rev. B* **84** 134516
- [45] Li J *et al* 2012 *Phys. Rev. B* **85** 214509
- [46] Golubov A A and Mazin I I 1997 *Phys. Rev. B* **55** 15146–52
- [47] Ummarino G 2007 *J. Supercond. Nov. Magn.* **20** 639–42
- [48] Senga Y and Kontani H 2008 *J. Phys. Soc. Japan* **77** 113710
- [49] Onari S and Kontani H 2009 *Phys. Rev. Lett.* **103** 177001
- [50] Efremov D V, Korshunov M M, Dolgov O V, Golubov A A and Hirschfeld P J 2011 *Phys. Rev. B* **84** 180512
- [51] Efremov D V, Golubov A A and Dolgov O V 2013 *New J. Phys.* **15** 013002
- [52] Wang Y, Kreisel A, Hirschfeld P J and Mishra V 2013 *Phys. Rev. B* **87** 094504
- [53] Korshunov M M, Efremov D V, Golubov A A and Dolgov O V 2014 *Phys. Rev. B* **90** 134517
- [54] Yao Z J, Chen W Q, Li Y K, Cao G H, Jiang H M, Wang Q E, Xu Z A and Zhang F C 2012 *Phys. Rev. B* **86** 184515
- [55] Chen H, Tai Y Y, Ting C S, Graf M J, Dai J and Zhu J X 2013 *Phys. Rev. B* **88** 184509
- [56] Castellani C, Natoli C R and Ranninger J 1978 *Phys. Rev. B* **18** 4945–66
- [57] Oleś A M 1983 *Phys. Rev. B* **28** 327–39
- [58] Berk N F and Schrieffer J R 1966 *Phys. Rev. Lett.* **17** 433–5
- [59] Allen P B and Mitrovic B 1982 *Theory of superconducting T_c (Solid State Physics: Advances in Research and Applications vol. 37)* ed H Erenreich, F Zeitz and D Turnbull (New York: Academic) pp 1–92
- [60] Parker D, Dolgov O V, Korshunov M M, Golubov A A and Mazin I I 2008 *Phys. Rev. B* **78** 134524
- [61] Popovich P, Boris A V, Dolgov O V, Golubov A A, Sun D L, Lin C T, Kremer R K and Keimer B 2010 *Phys. Rev. Lett.* **105** 027003
- [62] Charnukha A, Dolgov O V, Golubov A A, Matiks Y, Sun D L, Lin C T, Keimer B and Boris A V 2011 *Phys. Rev. B* **84** 174511